JOURNAL OF AIRCRAFT
Vol. 42, No. 2, March–April 2005

Autonomous Coordination of Aircraft Formations Using Direct and Nearest-Neighbor Approaches

L. Silverberg* and B. A. Levedahl†
North Carolina State University, Raleigh, North Carolina 27695-7901

Two approaches are developed for autonomous coordination of aircraft formations. The development of the approaches relies on past work in the areas of distributed control (modal, robust, optimal, and decentralized). The formation coordination problem is divided into a tracking problem (changing the formation) and a regulation problem (maintaining the formation). How to separate the spatial parts of the tracking problem from the temporal parts is demonstrated. With respect to the regulation problem, it is shown that the goal of the regulation problem is to dampen uniformly the motion of the aircraft. It is pointed out that for fuel-optimality the closed-loop damping factors of the aircraft need to be less than $\pi/2$. Two types of decentralized coordination are examined: direct coordination (using inertial measurements) and nearest-neighbor coordination (using relative measurements). A perturbation analysis is developed for the efficient calculation of control gains that minimize power and uniformly dampen motion. A numerical example illustrates robust formation changes from nine-aircraft (3×3) grids to V-type formations. Why the performance of direct coordination is generally better than the performance of nearest-neighbor coordination and why implementing direct coordination is simpler than implementing nearest-neighbor coordination are explained. However, nearest-neighbor coordination can be used in collision avoidance, and so it must still be considered as a viable option.

I. Introduction

THE autonomous coordination of aircraft formations is an upcoming control problem of growing importance in the aerospace industry. The problem represents a relatively new application to fundamental issues in distributed control, sensing, and electronics. The strategies being employed to solve this control problem build on the already strong foundations that exist in several primary areas of distributed control, namely, modal control, robust control, decentralized control, and optimal control. Pioneering work in modal control was performed by Balas[1] in 1978 and by Meirovitch and Baruh[2] in 1982. A strong framework for robust control of self-adjoint, distributed-parameter systems was developed by Arbel and Gupta[3] in 1981 and by Hale and Rahn[4] in 1984, and the robust control problem was applied to modal control by Baruh and Silverberg[5] in 1985. Calico and Miller[6] in 1983 were among the first to formulate the decentralized control problem for self-adjoint distributed systems.

An important outcome of the research in distributed control during the 1970s and 1980s was the recognition that modal control, optimal control, decentralized control, and robust control were not necessarily conflicting objectives. Modal control was formulated as a globally optimal control problem by Meirovitch and Silverberg[7] in 1986, and the first-order approximation to this globally optimal control problem was shown to be decentralized by Silverberg[8] in 1985. This mutually optimal, modal, decentralized, and robust control was examined in more detail by Silverberg and Morton[9] in 1989, by Silverberg[10] in 1990, and by Silverberg et al.[11] in 1992. The application of these results to maneuvering spacecraft was developed by Baruh and Silverberg[12] in 1988 and by Silverberg and Foster[13] in 1990. It was shown that the mutually optimal, modal, decentralized, robust control indicated earlier could uniformly dampen and uniformly stiffen the modes of vibration of the distributed system by Silverberg and Washington[14,15] in 1997 and 1999.

Received 4 December 2003; revision received 20 May 2004; accepted for publication 22 May 2004.

*Professor, Department of Mechanical and Aerospace Engineering.
†Graduate Research Assistant, Department of Mechanical and Aerospace Engineering. Student Member AIAA.

The application of decentralized control to autonomous formations has received considerable attention. Wolfe et al. used a vortex lattice method and decentralized regulation of a three-plane V formation.[16] The recalculation of the stability derivatives in tight formations was considered by Pachter et al.[17] Richards et al. treated the multiple unmanned aerial vehicle (UAV) task allocation and trajectory planning problem using a single mixed-integer linear programming approach and a trajectory planning approximation approach.[18] Bellingham et al. investigated the problem of UAV fleet cooperative path planning.[19] Mehiel and Balas investigated the exponential stability of swarm formations using two-dimensional discrete-time, nonlinear, logic-based control algorithms.[20] On the implementation side, Olsen et al. advanced differential carrier-phase global positioning system (GPS) sensing by developing two lighter-than-air vehicles and performing coordinated maneuvers with them.[21] On the aerodynamics side, Frazier and Gopalarathnam developed a theory on optimal wing lift distributions for aircraft flying in formation.[22]

This paper presents two basic decentralized strategies for autonomous coordination (tracking and regulation) of aircraft formations. The strategies developed in this paper place an emphasis on separating the problem into independent effects at the controls, sensors, and electronics levels, to the extent possible. The first strategy employs inertial measurements and is termed direct coordination. The second strategy employs relative measurements and is termed nearest-neighbor coordination.

In Sec. II the aircraft formation dynamics are described, and in Sec. III, the connectivity between aircraft is discussed. In Sec. IV, the coordination and control problem is set up. In Sec. V, issues associated with changing the formation are addressed, and in Sec. VI, the problem of maintaining the formation is formulated. The direct coordination problem and the nearest-neighbor coordination problem are formulated in that section. In Sec. VII, a numerical example is presented that brings out basic features of the autonomous coordination problem, and in Sec. VIII the paper is summarized and conclusions are given.

II. Aircraft Formation Dynamics

The motion of the ith aircraft is governed by the six equations of motion,

$$m^{(i)}\boldsymbol{A}^{(i)} = \boldsymbol{F}^{(i)}, \qquad i = 1, 2, \ldots, n \tag{1a}$$

$$I^{(i)}\dot{\boldsymbol{\Omega}}^{(i)} + \boldsymbol{\Omega}^{(i)} \times I\boldsymbol{\Omega}^{(i)} = \boldsymbol{M}^{(i)} \tag{1b}$$

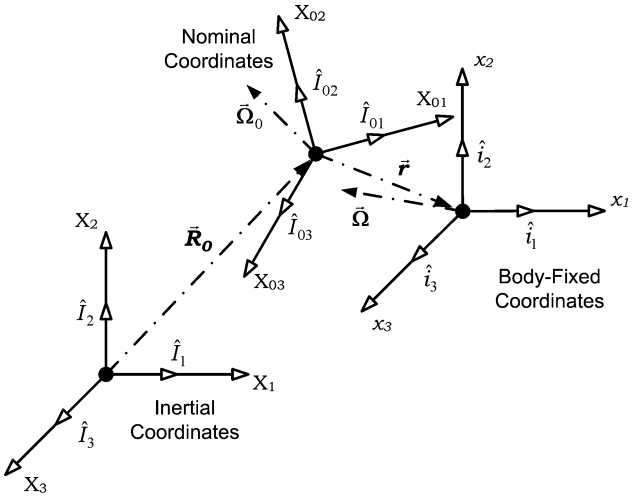

Fig. 1 Formation coordinate system.

in which $m^{(i)}$ is mass, $\boldsymbol{F}^{(i)}$ is the external force, $I^{(i)}$ is the inertia matrix about the mass center, $\boldsymbol{\Omega}^{(i)}$ is the angular velocity, $\boldsymbol{M}^{(i)}$ is the control moment about the mass center in which three-dimensional vectors are indicated in bold and where the overdot represents a differentiation in the tracking coordinates shown in Fig. 1.

Let us express the position of the mass center, the external force, and the external moment as $\boldsymbol{R}^{(i)} = \boldsymbol{R}_0^{(i)} + \boldsymbol{r}^{(i)}$, $\boldsymbol{F}^{(i)} = \boldsymbol{F}_0^{(i)} + \boldsymbol{f}^{(i)}$, and $\boldsymbol{M}^{(i)} = \boldsymbol{M}_0^{(i)} + \boldsymbol{m}^{(i)}$ in which nominal quantities are indicated by the subscript 0 and perturbed quantities are expressed in terms of nominal coordinates. The velocities and accelerations are then $\boldsymbol{V}^{(i)} = \boldsymbol{V}_0^{(i)} + \boldsymbol{v}^{(i)}$ and $\boldsymbol{A}^{(i)} = \boldsymbol{A}_0^{(i)} + \boldsymbol{a}^{(i)}$ in which $\boldsymbol{a}^{(i)} = \dot{\boldsymbol{v}}^{(i)} + \boldsymbol{\Omega}^{(i)} \times \boldsymbol{v}^{(i)}$. When small perturbations are assumed, the angular velocity is $\boldsymbol{\Omega}^{(i)} = \boldsymbol{\Omega}_0^{(i)} + \boldsymbol{\omega}^{(i)}$, where $\boldsymbol{\omega}^{(i)} = \dot{\boldsymbol{\theta}}^{(i)}$ in which $\boldsymbol{\theta}$ is a three-dimensional vector of Euler angles. Substituting these relationships into Eq. (1) yields the nonlinear equations governing the motion of the nominal system

$$m^{(i)}\boldsymbol{A}_0^{(i)} = \boldsymbol{F}_0^{(i)}, \qquad i = 1, 2, \ldots, n \tag{2a}$$

$$I^{(i)}\dot{\boldsymbol{\Omega}}_0^{(i)} + \boldsymbol{\Omega}_0^{(i)} \times I\boldsymbol{\Omega}_0^{(i)} = \boldsymbol{M}_0^{(i)} \tag{2b}$$

and the linear equations governing the perturbed system

$$m^{(i)}\left(\dot{\boldsymbol{v}}^{(i)} + \boldsymbol{\Omega}_0^{(i)} \times \boldsymbol{v}^{(i)}\right) = \boldsymbol{f}^{(i)}, \qquad i = 1, 2, \ldots, n \tag{3a}$$

$$I^{(i)}\dot{\boldsymbol{\omega}}^{(i)} + \boldsymbol{\Omega}_0^{(i)} \times I\boldsymbol{\omega}^{(i)} + \boldsymbol{\omega}^{(i)} \times I\boldsymbol{\Omega}_0^{(i)} = \boldsymbol{m}^{(i)} \tag{3b}$$

in which the nonlinear terms $\boldsymbol{\omega}^{(i)} \times \boldsymbol{v}^{(i)}$ and $\boldsymbol{\omega}^{(i)} \times I\boldsymbol{\omega}^{(i)}$ have been neglected. These two nonlinear terms can be neglected based on the assumption that the angular rates are small (The vehicles are typically rotating but not spinning). Notice that Eqs. (2a) and (3a) govern the translational motion of the aircraft, both the nominal and the perturbed parts, and that Eqs. (2b) and (3b) govern the rotational motion of the aircraft, both the nominal and the perturbed parts.

The external forces and the external moments are created by weight, aerodynamic control surfaces, and thrust, written

$$\boldsymbol{F}_0^{(i)} = \boldsymbol{F}_{0W}^{(i)} + \boldsymbol{F}_{0A}^{(i)} + \boldsymbol{F}_{0\mathrm{Th}}^{(i)} \tag{4a}$$

$$\boldsymbol{M}_0^{(i)} = \boldsymbol{M}_{0W}^{(i)} + \boldsymbol{M}_{0A}^{(i)} + \boldsymbol{M}_{0\mathrm{Th}}^{(i)} \tag{4b}$$

$$\boldsymbol{f}^{(i)} = \boldsymbol{f}_W^{(i)} + \boldsymbol{f}_A^{(i)} + \boldsymbol{f}_{\mathrm{Th}}^{(i)} \tag{4c}$$

$$\boldsymbol{m}^{(i)} = \boldsymbol{m}_W^{(i)} + \boldsymbol{m}_A^{(i)} + \boldsymbol{m}_{\mathrm{Th}}^{(i)} \tag{4d}$$

in which W, A, and Th denote the weight, aerodynamic, and thrust components. The aerodynamic forces and the thrust depend on the aileron angles, elevator angles, rudder angles, and throttle setting, which are collected into the input vector $\boldsymbol{\Delta}^{(i)} = \boldsymbol{\Delta}_0^{(i)} + \boldsymbol{\delta}^{(i)}$. The functional dependence of the aerodynamic forces is expressed as

$$\boldsymbol{F}_{0A}^{(i)} = \boldsymbol{F}_{0A}^{(i)}\left(\boldsymbol{V}_0^{(i)}, \dot{\boldsymbol{V}}_0^{(i)}, \boldsymbol{\Theta}_0^{(i)}, \boldsymbol{\Omega}_0^{(i)}, \dot{\boldsymbol{\Omega}}_0^{(i)}, \boldsymbol{\Delta}_0^{(i)}, \dot{\boldsymbol{\Delta}}_0^{(i)}, \ddot{\boldsymbol{\Delta}}_0^{(i)}\right) \tag{5a}$$

$$\boldsymbol{M}_{0A}^{(i)} = \boldsymbol{M}_{0A}^{(i)}\left(\boldsymbol{V}_0^{(i)}, \dot{\boldsymbol{V}}_0^{(i)}, \boldsymbol{\Theta}_0^{(i)}, \boldsymbol{\Omega}_0^{(i)}, \dot{\boldsymbol{\Omega}}_0^{(i)}, \boldsymbol{\Delta}_0^{(i)}, \dot{\boldsymbol{\Delta}}_0^{(i)}, \ddot{\boldsymbol{\Delta}}_0^{(i)}\right) \tag{5b}$$

$$\boldsymbol{f}_A^{(i)} = \boldsymbol{f}_A^{(i)}\left(\boldsymbol{V}_0^{(i)}, \dot{\boldsymbol{V}}_0^{(i)}, \boldsymbol{\Theta}_0^{(i)}, \boldsymbol{\Omega}_0^{(i)}, \dot{\boldsymbol{\Omega}}_0^{(i)}, \boldsymbol{\Delta}_0^{(i)}, \dot{\boldsymbol{\Delta}}_0^{(i)}, \ddot{\boldsymbol{\Delta}}_0^{(i)}, \boldsymbol{v}^{(i)}, \dot{\boldsymbol{v}}, \boldsymbol{\theta}^{(i)}, \boldsymbol{\omega}^{(i)}, \dot{\boldsymbol{\omega}}^{(i)}, \boldsymbol{\delta}^{(i)}, \dot{\boldsymbol{\delta}}^{(i)}, \ddot{\boldsymbol{\delta}}^{(i)}\right) \tag{5c}$$

$$\boldsymbol{m}_A^{(i)} = \boldsymbol{m}_A^{(i)}\left(\boldsymbol{V}_0^{(i)}, \dot{\boldsymbol{V}}_0^{(i)}, \boldsymbol{\Theta}_0^{(i)}, \boldsymbol{\Omega}_0^{(i)}, \dot{\boldsymbol{\Omega}}_0^{(i)}, \boldsymbol{\Delta}_0^{(i)}, \dot{\boldsymbol{\Delta}}_0^{(i)}, \ddot{\boldsymbol{\Delta}}_0^{(i)}, \boldsymbol{v}^{(i)}, \dot{\boldsymbol{v}}, \boldsymbol{\theta}^{(i)}, \boldsymbol{\omega}^{(i)}, \dot{\boldsymbol{\omega}}^{(i)}, \boldsymbol{\delta}^{(i)}, \dot{\boldsymbol{\delta}}^{(i)}, \ddot{\boldsymbol{\delta}}^{(i)}\right) \tag{5d}$$

and the functional dependence of the thrust forces is

$$\boldsymbol{F}_{0\mathrm{Th}}^{(i)} = \boldsymbol{F}_{0\mathrm{Th}}^{(i)}\left(\boldsymbol{\Delta}_0^{(i)}, \dot{\boldsymbol{\Delta}}_0^{(i)}, \ddot{\boldsymbol{\Delta}}_0^{(i)}\right) \tag{6a}$$

$$\boldsymbol{M}_{0\mathrm{Th}}^{(i)} = \boldsymbol{M}_{0\mathrm{Th}}^{(i)}\left(\boldsymbol{\Delta}_0^{(i)}, \dot{\boldsymbol{\Delta}}_0^{(i)}, \ddot{\boldsymbol{\Delta}}_0^{(i)}\right) \tag{6b}$$

$$\boldsymbol{f}_{\mathrm{Th}}^{(i)} = \boldsymbol{f}_{0\mathrm{Th}}^{(i)}\left(\boldsymbol{\Delta}_0^{(i)}, \dot{\boldsymbol{\Delta}}_0^{(i)}, \ddot{\boldsymbol{\Delta}}_0^{(i)}, \boldsymbol{\delta}^{(i)}, \dot{\boldsymbol{\delta}}^{(i)}, \ddot{\boldsymbol{\delta}}^{(i)}\right) \tag{6c}$$

$$\boldsymbol{m}_{\mathrm{Th}}^{(i)} = \boldsymbol{m}_{0\mathrm{Th}}^{(i)}\left(\boldsymbol{\Delta}_0^{(i)}, \dot{\boldsymbol{\Delta}}_0^{(i)}, \ddot{\boldsymbol{\Delta}}_0^{(i)}, \boldsymbol{\delta}^{(i)}, \dot{\boldsymbol{\delta}}^{(i)}, \ddot{\boldsymbol{\delta}}^{(i)}\right) \tag{6d}$$

where $\boldsymbol{\Theta}_0^{(i)}$ are the Euler angles associated with the nominal coordinates. Notice in Eq. (5a) that the dependence of the nominal aerodynamic force is traditionally represented as a product of $\frac{1}{2}\rho V_\infty^2 S$ multiplied by a sum of aerodynamic force coefficients and similarly that Eq. (5b) is represented as a product of $\frac{1}{2}\rho V_\infty^2 Sb$ multiplied by a sum of aerodynamic moment coefficients. A similar representation is used for Eqs. (6a) and (6b).

The closed-loop aircraft system has been divided into a nominal system represented by Eqs. (2a), (2b), (5a), (5b), (6a), and (6b) and a perturbed system represented by Eqs. (3a), (3b), (5c), (5d), (6c), and (6d). The nominal aircraft system is a decoupled set of blocks of equations associated with each aircraft. The nominal dynamics of the individual aircraft is neither coupled by the other aircraft nor affected by the perturbations. Furthermore, the nominal quantities in Eqs. (5c), (5d), (6c), and (6d), given that their stability characteristics are independent of the perturbations, act as disturbances on the perturbed system. They, too, do not affect the stability characteristics of the perturbed system. However, depending on the method of autonomous control, the stability characteristics of the individual aircraft can be coupled, necessitating the stability characteristics of the entire formation to be studied.

III. Connectivity Between Aircraft

In view of the preceding section, the coupling between aircraft in the formation drives the stability of the formation. Thus, the question arises as to the different ways aircraft can be connected, the issues associated with the different types of connections, and their impact on aircraft stability.

A network for autonomously flying aircraft consists of wireless communication signals and wireless measurement signals. The communication signals are characteristically intermittent, and they can be transmitted and received with relatively low bandwidth requirements. The measurement signals are characteristically continuous in time analog signals that require more stringent requirements in speed and bandwidth. There are two types of measurement signals of interest in formation flying: relative measurements, which are between aircraft, and inertial measurements, which are between the aircraft and the reference source, for example, ground and GPS.

The measurement process is essentially a triangulation process. Robust triangulation is best accomplished by separating the transmitters from the receivers. Well-separated transmitters during transmission and well-separated receivers during reception maximize robustness in the presence of sensor noise. For example, inertial

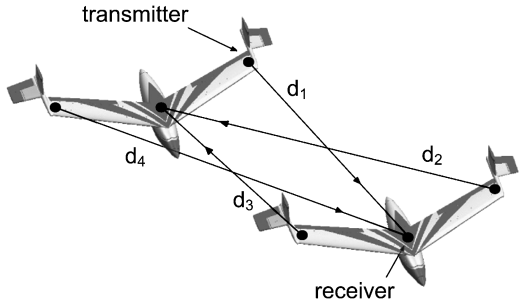

Fig. 2 Sensing truss.

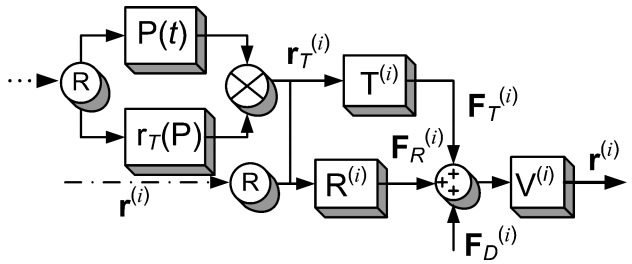

a) Direct (inertial)

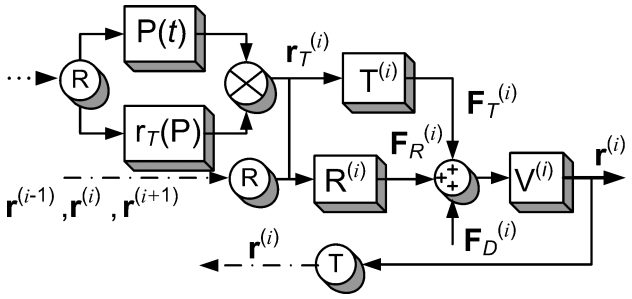

b) Nearest neighbor (relative)

Fig. 3 Block diagram for direct and nearest-neighbor vehicle coordination: $V^{(i)}$, vehicle dynamics; $T^{(i)}$, tracking controller; $R^{(i)}$, regulation controller; $P(t)$, temporal functional; $r_T(P)$, spatial functional; ——, hardwired signals; - - - -, wireless communication; —·—, wireless measurement; Ⓡ, receiver; and Ⓣ, transmitter.

measurements of aircraft are received from GPS satellite transmitters that are well separated. If relative measurements are needed, the transmitters on the aircraft need to be well separated. In a planar system, two transmitters and one receiver on each of the ith and jth aircraft fully determine the relative position and orientation of the jth aircraft relative to the ith aircraft and the ith aircraft relative to the jth aircraft (Fig. 2). In a three-dimensional system, three transmitters and one receiver on each of the ith and jth aircraft fully determine the relative position and orientation of the jth aircraft relative to the ith aircraft and the ith aircraft relative to the jth aircraft (communications with V. Perez, System Programmer, Mechanical and Aerospace Engineering, North Carolina State University, Raleigh, North Carolina). The receiving signals and the transmitting signals for the measurement process make up a sensing truss, which possesses stability characteristics that are analogous to the stability characteristics of the corresponding structural truss (Fig. 2).

The complexity of the network is important, particularly in the event that failures occur. The methods and procedures for accommodating for failures grow in complexity with the complexity of the network. The question arises to what extent the complexity of the network can be minimized. The two simplest networks are direct networks and nearest-neighbor networks. Direct networks use inertial measurements on each aircraft, eliminating the need for relative measurements, all together. Nearest-neighbor networks designate at least one aircraft as the leader and the others as the followers. The leaders receive inertial measurements, and the leaders and the followers are linked by relative measurements. Direct and nearest-neighbor networks with one leader are developed in this paper.

Figure 3a shows a block-diagram representation for a direct network. As shown; the ith aircraft receives a wireless measurement of inertial position and a wireless communication from the reference source. The other elements of the block diagram will be described later. Figure 3b shows a block-diagram representation for a nearest-neighbor network. As shown, the ith aircraft receives wireless measurements from neighboring aircraft of relative position, transmits a reference signal to neighboring aircraft, and receives a wireless communication from an external command source. If the ith aircraft is the leader, a wireless measurement of inertial position is also received (not shown).

IV. Aircraft Coordination and Control

The aircraft formation problem can be partitioned into two separate parts: coordination and control. The coordination is the first level in a two-level hierarchy and is responsible for controlling the global degrees of freedom (position and orientation) of each of the aircraft through the resultant external forces and resultant external moments. The second level of the hierarchy is an aircraft control problem and is responsible for the conversion of resultant external forces and resultant external moments into control forces and control moments. Flight constraints that limit achievable global degrees of freedom and achievable control forces and control moments are also imposed at the second level of the hierarchy. This paper pertains to the first level of the hierarchy, which is largely independent of the aircraft type, in contrast with the second level of the hierarchy, which is aircraft specific.

The aircraft formation problem is formulated much like the way the aircraft vehicle control problems are formulated. The coordination of the formation is separated into the problem of tracking the nominal formation (changing the formation) and the problem of regulating the perturbation in the formation (maintaining the formation).[23] This enables the task of changing a formation and the task of maintaining a formation to be separated into processes that are designed independently of each other. The implication is that the settling time, peak-overshoot, and steady-state error requirements of the regulation problem can be met independently of the formation change requirements.

At the coordination level of the hierarchy, the individual aircraft do not necessarily have to represent independent aircraft. They can be artificially coupled, producing, effectively, a mass–spring–damper system that exhibits its own dynamic characteristics. In this paper, the aircraft are treated both independently and as coupled mass–spring–damper systems to study the relative merits of these approaches. The aircraft formation problem that treats the aircraft independently is called the direct formation problem. It uses inertial measurements as described in the preceding section. The aircraft formation problem that treats the aircraft as coupled mass–spring–dampers is called the nearest-neighbor formation problem. It uses relative measurements as described in the preceding section.

In Eq. (4), recall that the control force and the control moment can be written as

$$\boldsymbol{F}^{(i)} = \boldsymbol{F}_0^{(i)} + \boldsymbol{f}^{(i)} \tag{7a}$$

$$\boldsymbol{M}^{(i)} = \boldsymbol{M}_0^{(i)} + \boldsymbol{m}^{(i)} \tag{7b}$$

The tracking forces and the tracking moments control formation changes, and the regulation forces and regulation moments maintain the formation.

V. Changing the Formation

In certain applications, the interest lies in developing autonomous formations with as many predetermined formations as possible. However, it is prohibitive to prerecord each possible formation change. To enable the aircraft to fly in a large number of possible formations, the formations can be generated onboard from a set of elementary formations. The formations would then be generated by superimposing elementary formations, translating and rotating the elementary formations, expanding them, etc. Figure 4a shows a translation and rotation of an elementary formation, and Fig. 4b

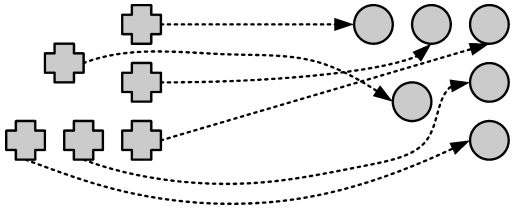

a) Translation and rotation

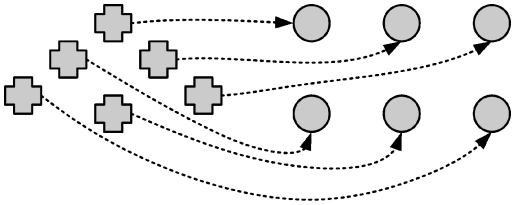

b) Configuration and density change

Fig. 4 Individual and global formation changes.

shows a configuration and density change of an elementary formation. The particular formations that are coordinated this way are expressed in terms of just a few parameters.

The tracking forces $\boldsymbol{F}_0^{(i)}$ and the tracking moments $\boldsymbol{M}_0^{(i)}$ in Eq. (7) cause the aircraft to follow the nominal paths $\boldsymbol{R}_0^{(i)}$ and $\boldsymbol{\Omega}_0^{(i)}$. Let us now separate the positions $\boldsymbol{R}_0^{(i)}$ into spatial and temporal components that can be designed independently of each other. This is accomplished by expressing the nominal position only implicitly as a function of time and explicitly as a function of space, written

$$\boldsymbol{R}_0^{(i)} = \boldsymbol{R}_0^{(i)}\left(P^{(i)}(t)\right) \tag{8}$$

in which $\boldsymbol{R}_0^{(i)}(P)$ is the spatial part and $P^{(i)}(t)$ is the temporal part. Differentiating Eq. (8) twice with respect to time yields

$$\boldsymbol{A}_0^{(i)} = \boldsymbol{R}_0^{\prime\prime(i)}\dot{P}^{2^{(i)}} + \boldsymbol{R}_0^{\prime(i)}\ddot{P}^{(i)} \tag{9}$$

where primes denote derivatives with respect to P and overdots represent derivatives with respect to t. Equation (9) is substituted into Eq. (2a) for the generation of the tracking forces. The separation of the tracking force into spatial and temporal parts simplifies the coordination architecture of the formation. This separation enables the temporal aspects of the formation change, for example, rapid/slow, to be separated from the spatial aspects of the formation change, for example, particular initial formation and final formation, reducing the onboard formation data to a listing of elementary formations.

For example, in a straight formation change, Eq. (8) becomes

$$\boldsymbol{R}_0^{(i)}(P) = \mu^{(i)}\boldsymbol{R}_1^{(i)} + \tau^{(i)}\boldsymbol{R}_2^{(i)} \tag{10a}$$

$$\mu^{(i)} + \tau^{(i)} = 1 \tag{10b}$$

$$P(t) = 3(t/T)^2 - 2(t/T)^3 \tag{10c}$$

in which $\boldsymbol{R}_1^{(i)} = [x_1^{(i)}\ \ y_1^{(i)}\ \ z_1^{(i)}]^T$ and $\boldsymbol{R}_2^{(i)} = [x_2^{(i)}\ \ y_2^{(i)}\ \ z_2^{(i)}]^T$ are the initial position and the final position of the ith aircraft in the formations and where T is the period of the formation change. Equations (10a) and (10b) prescribe the spatial part of the formation change separate from the temporal part, which is prescribed by Eq. (10c).

For the purposes of collision avoidance, it can become necessary during the formation change to follow paths that are not straight. For example, a suitable parameterized planar parabolic formation change is given by (Fig. 5)

$$\boldsymbol{R}_0^{(i)}(P) = \boldsymbol{R}_1^{(i)} + \begin{bmatrix} x_2^{(i)} - x_1^{(i)} & y_1^{(i)} - y_2^{(i)} & 0 \\ y_2^{(i)} - y_1^{(i)} & x_2^{(i)} - x_1^{(i)} & 0 \\ 0 & 0 & 1 \end{bmatrix} \begin{pmatrix} P \\ 4qP(1-P) \\ 0 \end{pmatrix}$$

$$0 \le P \le 1 \tag{11}$$

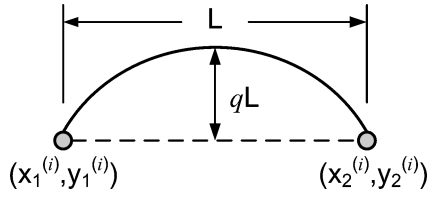

Fig. 5 Planar parabolic formation change.

where q is parabolic eccentricity, which represents the ratio of the height to the length of the parabolic path. Notice that the spatial and temporal separation enables the designer to prescribe the spatial path of each aircraft, given by Eqs. (10a) and (10b) or by Eq. (11), independent of the temporal changes, given by Eq. (10c).

Once the nominal path $\boldsymbol{R}_0^{(i)}$ is prescribed, the nominal orientation $\boldsymbol{\Theta}_0^{(i)}$ follows as a constraint. In fact, the aircraft control inputs (at the second level of the hierarchy) generate the orientation and the path in Eqs. (2a) and (2b).

VI. Maintaining the Formation

The general regulation problem is a non-full-dimensional control problem in which the number of control inputs is less than the number of degrees of freedom (translational and rotational). Never the less, when the aircraft is sufficiently maneuverable, the rotational degrees of freedom can be prescribed sufficiently fast to enable the aircraft to follow any desirable nominal path, at least in theory. In such cases, the aircraft formation can be regarded as a mass–spring–damper system at the first level of the hierarchy, decoupled from the rotational problem associated with rotational inertia. The aircraft formation problem, in this case, is associated with the translational motion of the aircraft, which is described in Eqs. (3a). Equation (3a) is rewritten as

$$m^{(i)}\ddot{\boldsymbol{r}}^{(i)} = \boldsymbol{f}^{(i)} - m^{(i)}\left[\dot{\boldsymbol{\Omega}}_0^{(i)} \times \boldsymbol{r}^{(i)} + 2\boldsymbol{\Omega}_0^{(i)} \times \dot{\boldsymbol{r}}^{(i)} + \boldsymbol{\Omega}_0^{(i)} \times \left(\boldsymbol{\Omega}_0^{(i)} \times \boldsymbol{r}^{(i)}\right)\right] \tag{12}$$

The right side of Eq. (12) represents a full-dimensional regulation force vector $\boldsymbol{f}_R$, where the terms in brackets are negligible when the angular velocities of the nominal system are sufficiently small (although that is not necessary).

The regulation problem can be formulated as an optimal control problem, as a direct control problem, as an independent modal space control problem, or as a robust control problem.[23] Regardless of the manner in which the problem is formulated, it has been shown that an effective full-dimensional control problem can be formulated that is direct, with modes that are controlled independently of the other, with insensitivity to errors in the physical parameters, and with dynamic performance that is globally optimal.[8] The globally optimal solution uniformly dampens the system. These results also suggest that the aircraft formation problem should be formulated either as a direct coordination problem or as a nearest-neighbor coordination problem, depending on the types of sensors that are used. The question arises as to their relative merits.

Direct coordination can be implemented when each aircraft is equipped with inertial sensors, and nearest-neighbor coordination can be implemented when one or more of the aircraft (the leaders) is equipped with inertial measurements and the remaining aircraft (the followers) are equipped with relative measurements. Because nearest-neighbor coordination uses relative measurements, and because relative measurements can also be used for collision avoidance, nearest-neighbor coordination represents an important option to consider.

Direct Coordination

The use of direct coordination raises questions associated with the global behavior of the formation and the fuel optimality of the coordination, given that direct coordination is a constrained form of coupled coordination. It has been shown in the earlier cited references, however, that uniform damping of the associated modes of

vibration of a mass–spring–damper system can be implemented in a direct manner, that uniform damping is fuel optimal, and that uniform damping does not require knowledge of the modal behavior of the system. In the case of aircraft formation coordination, because the control actuation is mapped to the desired movement through control surface deflections, the fuel optimality constraint minimizes the control surface movements and reduces extreme aircraft movements to maintain formation. The control algorithms associated with uniform damping can also be expressed in terms of just a few parameters.

First consider the direct implementation of uniform damping. The uniform damping and stiffening algorithm is[14]

$$\boldsymbol{f}_R^{(i)} = -2\alpha m^{(i)}\dot{\boldsymbol{r}}^{(i)} - (\alpha^2+\beta^2)m^{(i)}\boldsymbol{r}^{(i)} \tag{13}$$

in which α is the uniform closed-loop decay rate of the ith aircraft and β is the uniform closed-loop frequency of oscillation of the ith aircraft. The closed-loop decay rates can be selected to dampen 90% of the error over the settling time T_s, in which case the closed-loop decay rate is expressed in terms of the settling time as $\alpha = \ell_n(10)/T_s$. The closed-loop response of the ith aircraft is then

$$\boldsymbol{r}^{(i)} = e^{-\alpha t}\left\{\boldsymbol{r}_0^{(i)}\cos(\beta t) + (1/\beta)\left[\dot{\boldsymbol{r}}_0^{(i)} + \alpha\boldsymbol{r}_0^{(i)}\right]\sin(\beta t)\right\} \tag{14}$$

When the settling time is held constant, it can be shown that the control effort

$$C^{(i)} = \int_0^\infty \left|\boldsymbol{f}_R^{(i)}\right|^2 \mathrm{d}t$$

associated with the ith aircraft is minimized when $\beta T_s = \pi/2$. This solution does not take into account the desire to control peak overshoot. Peak overshoot requirements can further increase the closed-loop frequency β of the ith aircraft, depending on the admissible set of disturbances. It follows that the optimal responses of aircraft flying in a formation are underdamped and that $\alpha/\beta = 2\,\ell_n(10)/\pi \cong 1.5$ provides an upper bound. The direct coordination problem formulated earlier is also extremely robust. It can be shown that the stability of the aircraft is independent of the physical properties of the aircraft.

Nearest-Neighbor Coordination

When nearest-neighbor coordination is used, the designer's first task is to specify the connectivity between the aircraft, that is, its nearest neighbors. Furthermore, the designer needs to specify the leaders and the followers. The leaders are the aircraft equipped with inertial measurements. The followers are equipped with relative measurements between nearest neighbors (connectivity). Consider the case in which there is one leader. Let the leader be designated by the subscript 1 and the followers designated by the subscripts $2, 3, \ldots, 3n$. The associated connectivity matrix is $\boldsymbol{C}(i, j), i, j = 1, \ldots, 3n$, in which the ith row is associated with the ith aircraft, the jth entry in the ith row is 1 (or 0) if the jth aircraft can (or can not) measure relative to the ith aircraft. The number of 1s in the matrix represents the number of one-way connections. Note that it is not necessary that $\boldsymbol{C}$ be symmetric, that is, a designer can design a jth aircraft that can measure relative to the ith aircraft, whereas the ith aircraft can not measure relative to the jth aircraft, for example, aircraft that can only see ahead and not behind. However, when $\boldsymbol{C}$ is symmetric, the connections are each two-way and the feedback emulates a mass–spring–damper system. The nearest-neighbor linear regulation algorithm can be expressed as

$$\boldsymbol{f}_R = -G_R\boldsymbol{r} - H_R\dot{\boldsymbol{r}} \tag{15}$$

in which $\boldsymbol{r} = [\boldsymbol{r}^{(1)T}\ \boldsymbol{r}^{(2)T}\ \ldots\ \boldsymbol{r}^{(n)T}]^T$ is the configuration vector of the formation, $\boldsymbol{f}_R = [\boldsymbol{f}_R^{(1)T}\ \boldsymbol{f}_R^{(2)T}\ \ldots\ \boldsymbol{f}_R^{(n)T}]^T$ is the coordination force vector of the formation, and G_R and H_R are $3n \times 3n$ symmetric displacement gain and velocity gain matrices. In two dimensions, G_R and H_R are $2n \times 2n$.

The aircraft can be connected in a variety of ways; the best way to connect the aircraft is a matter of optimization. The connectivity matrix is associated with a specific pair of initial and final formations, each of which could be constructed from elementary formations, as developed earlier. For a given pair of initial and final formations, another consideration is associated with the stiffness of the associated connectivity. Because a follower is connected to the leader through more intermediary aircraft, its inertial position is known less directly, and the control of the motion of that aircraft based on relative information becomes more and more difficult. To circumvent this problem, the number of connections between the aircraft can be increased and/or the number of leaders can be increased. Of course, an increase in the number of connections and an increase in the number of leaders accompany increases in measurement complexity.

Substituting Eq. (15) into Eqs. (12) yields the closed-loop system,

$$M\ddot{\boldsymbol{r}} + H_R\dot{\boldsymbol{r}} + G_R\boldsymbol{r} = \boldsymbol{0} \tag{16}$$

in which M is the symmetric mass matrix of the formation. The symmetric nearest-neighbor coordination problem just formulated is extremely robust. It can be shown that global stability of the aircraft is guaranteed for positive control gains, independent of the physical properties of the aircraft.

Perturbation Analysis for Nearest-Neighbor Coordination

The question arises how to select the control gains in Eq. (16). The goal is to select control gains that uniformly dampen the motion to the extent possible, recognizing that uniform damping of the modes minimizes the required control authority of the actuation and maximizes the global dynamic performance of the formation. The nearest-neighbor control is constrained by the connectivity, which complicates the problem. To overcome this, first express the control gains as

$$G_R = \sum_{k=1}^{N} g_k B_k \tag{17a}$$

$$H_R = \sum_{k=1}^{N} h_k B_k \tag{17b}$$

in which g_k and h_k, $k = 1, 2, \ldots, N$, are positive control gains, N is the number of connections, and B_k is the $3n \times 3n$ connectivity matrix associated with the kth two-way connection. Stability is guaranteed provided $g_k > 0$ and $h_k > 0$ regardless of the physical parameters of the aircraft.

A first-order perturbation analysis is now used to calculate accurately the control gains. The eigenvalue problem associated with Eq. (16) is $[s_r^2 M + s_r H_R + G_R]\boldsymbol{\varphi}_r = 0$, in which s_r is the rth system eigenvalue and $\boldsymbol{\varphi}_r$ is the rth system eigenvector. The eigenquantities can be expressed as[24]

$$s_r = s_{0j} + s_{1j}, \qquad \boldsymbol{\varphi}_j = \boldsymbol{\varphi}_{0j} + \boldsymbol{\varphi}_{1j}$$
$$G_R = G_{R0}, \qquad H_R = H_{R1} \tag{18}$$

in which 0 denotes a nominal quantity and 1 indicates a perturbation (not to be confused with nominal quantities and perturbed quantities associated with the aircraft). The displacement gain matrix is regarded as a nominal quantity and the velocity control gain matrix is regarded as a perturbation. The nominal system becomes the symmetric mass–spring system, and the perturbed system includes the damping. This division of responsibilities enables the peak-overshoot requirements and the settling-time requirements in the nearest-neighbor coordination problem to be separated. The displacement control gain matrix is first determined to satisfy the peak-overshoot requirements followed by the determination of the velocity control gain matrix to satisfy the settling-time requirements, which will be done momentarily. Substituting the eigenquantities in Eq. (18) into the eigenvalue problem, premultiplying the result by $\boldsymbol{\varphi}_{0i}^T$, invoking the modal orthonormality conditions ($\boldsymbol{\varphi}_{0i}^T M\boldsymbol{\varphi}_{0j} = \delta_{ij}$ and $\boldsymbol{\varphi}_{0i}^T G_R\boldsymbol{\varphi}_{0j} = \beta_r^2\delta_{ij}$), and neglecting second- and higher-order terms yields

$$\alpha_i = \tfrac{1}{2}\boldsymbol{\varphi}_{0i}^T H_R\boldsymbol{\varphi}_{0i} \tag{19}$$

in which $s_{0i} = i\beta$ and $s_{1i} = -\alpha_i$ so that α_i is the closed-loop decay rate of the ith mode of the system. Equation (19) is a set of linear algebraic equations. The number of equations is equal to the number of degrees of freedom $3n$ ($2n$ for two-dimensional systems), and the number of unknowns N is equal to the number of connections. Substituting Eq. (17b) into Eq. (19) yields

$$\boldsymbol{\alpha} = D\boldsymbol{h} \tag{20a}$$

$$D_{ik} = \tfrac{1}{2}\boldsymbol{\varphi}_{0i}^T B_k \boldsymbol{\varphi}_{0i} \tag{20b}$$

in which $\boldsymbol{\alpha} = [\alpha_1 \ \alpha_2 \ \ldots \ \alpha_{3n}]^T$ is the $3n$-dimensional vector of approximate modal decay rates and $\boldsymbol{h} = [h_1 \ h_2 \ \ldots \ h_N]^T$ is the N-dimensional vector of velocity feedback gains that we wish to determine. In the following, the matrix D can be full rank or rank deficient without loss of generality. (If D is not full rank, the results can be modified using a singular-value decomposition, but for brevity this modification is omitted from the discussion.[25]) When the number of degrees of freedom is less than or equal to the number of connections and D is full rank, the weighted minimum norm solution of Eq. (20) is $\boldsymbol{h} = W^{-1}D^T(DW^{-1}D)^{-1}\boldsymbol{\alpha}$ in which W is an $N \times N$ weighting matrix and the weighted norm squared is $J = \boldsymbol{h}^T W \boldsymbol{h}$. When the number of equations is equal to the number of connections and D is full rank, a simple inverse of Eq. (20) yields the solution $\boldsymbol{h} = D^{-1}\boldsymbol{\alpha}$. When the number of degrees of freedom is greater than the number of connections and D is full rank, no exact solution to Eq. (20) exists, and we resort to approximate solutions. The case of more degrees of freedom than connections arises from the desire to limit the number of signals detected by the wireless receivers on the aircraft. There are several possible approximate solutions to Eq. (20) that can be obtained. The weighted least-squares solution, given by $\boldsymbol{h} = (D^T W D)^{-1} D^T W \boldsymbol{\alpha}$, minimizes the weighted error $e = (D\boldsymbol{h} - \boldsymbol{\alpha})^T W (D\boldsymbol{h} - \boldsymbol{\alpha})$. The weighting matrix W can be used to study different solutions. For example, a weighting matrix of the form $W = \mathrm{diag}(1, 2, 4, \ldots)$ would place more emphasis on the connections that are farther from the leader.

More than minimizing the error, solutions can be obtained that also penalize the deviation from uniform damping. Consider the functional

$$J = (\alpha\mathbf{1} - \boldsymbol{\alpha})^T W_\alpha (\alpha\mathbf{1} - \boldsymbol{\alpha}) + \boldsymbol{h}^T W_h \boldsymbol{h} \tag{21}$$

where $\mathbf{1} = [1 \ 1 \ \ldots \ 1]^T$, W_α is a $3n \times 3n$ weighting matrix associated with the non-uniformity of the decay rates and W_h is an $N \times N$ weighting matrix associated with the control effort. The first term in Eq. (21) is a penalty associated with nonuniform damping, and the second term penalizes the control effort. Minimization of Eq. (21) yields

$$\boldsymbol{h} = \alpha\left[D^T W_\alpha D + W_h\right]^{-1} D^T W_\alpha \mathbf{1} \tag{22}$$

Notice that Eq. (22) does not require that D be full rank, unlike the weighted minimum-norm solutions and the weight least-squares solutions given just after Eq. (20). This makes Eq. (22) particularly easy to use.

The control gains for nearest-neighbor coordination are determined in two independent steps. The displacement feedback gains are first determined based on peak-overshoot requirements (if any), and then the velocity feedback gains are determined based on settling-time requirements using Eq. (22).

VII. Numerical Example

The following example consists of a formation of nine aircraft that initially forms a planar 3×3 grid, and changes into a planar V-shaped formation. The number of degrees of freedom is 18 ($n = 9$). Each aircraft is an A-4D Skyhawk. The drag coefficient is $C_D = 0.03$, the Mach number is $M = 0.4$ (at sea level), the weight is $mg = 17{,}578$ lb, the wing span is $b = 27.5$ ft, and the wing area is $S = 260$ ft^2 (Ref. 26).

The tracking problem is first treated. Straight formation changes were first attempted, and aircraft 5 and 9 nearly collided during the formation change. Parabolic formation changes were then used, as shown in Fig. 6. To avoid collisions, the parabolic eccentricities were specified to be $q_1 = q_2 = q_3 = q_4 = q_6 = q_8 = 0$, $q_5 = -0.2$, $q_7 = -0.1$, and $q_9 = 0.1$. Although not performed here, the parabolic eccentricities could have been determined more optimally to maximize the separation between the aircraft over the time of the formation change and the lengths of the associated arcs. Also, notice that the actual paths of the aircraft and the desired paths of the aircraft are coincident in Fig. 6 because no disturbances have been introduced yet.

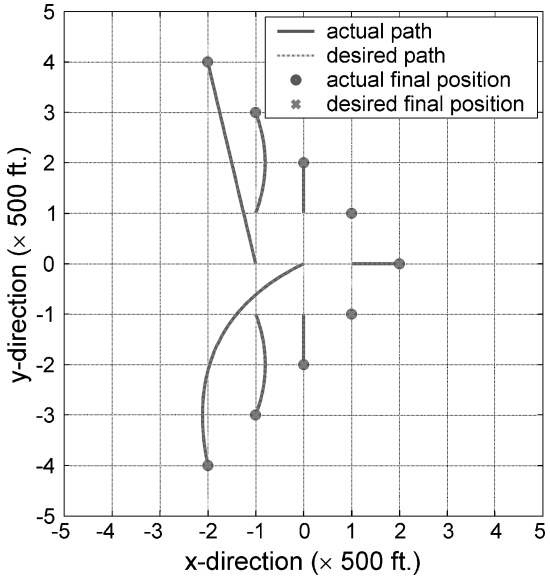

Fig. 6 Ideal open-loop formation change.

Next, a wind disturbance is introduced, and the combined tracking and regulation problem is treated. As mentioned earlier, the closed-loop frequency is determined by peak-overshoot requirements, which in turn depend on an admissible set of disturbances. For the purposes of this numerical example, assume that the separation distance in the 3×3 grid is $\Delta = 8b$ ($\approx$500 ft), that a strong initial wind gust changes the velocity of the aircraft by $v_w = 10$ kn ($0.0375M$), and that the minimum separation distance is required to be $(1 - \mu)\Delta = 450$ ft, where μ is a separation factor ($\mu = 0.1$). The period of the formation change was set to 30 s (where $\alpha = 0.0767$ rad/s), which corresponds to changes in aircraft velocities on the order of 45 kn. The settling time was set equal to the period of the formation change to reduce 90% of the tracking error by the time the formation change was completed.

Direct Coordination

Given the preceding parameters, the required closed-loop frequency associated with each aircraft is $\beta = v_w/(\mu\Delta) \approx 0.33$ rad/s. The closed-loop damping factor becomes $\alpha/\beta = 0.23$, which is less than the upper bound of 1.5. The control gains are given in Eq. (13) by $g = g^{(i)} = (\alpha^2 + \beta^2)m^{(i)} = 62.7$ lb/ft and $h = h^{(i)} = 2\alpha m^{(i)} = 83.8$ lb $\cdot$ s/ft. Figure 7 shows the formation change with an unusually large initial wind gust that changes the velocity of the aircraft by $v_w = 38$ kn at 45 deg occurring when the formation change was initiated. Notice that the overshoot of the error is within four times of $\mu\Delta$, as expected. The closed-loop eigenvalues are given in Table 1.

Nearest-Neighbor Network

The formation was connected using the connectivity shown in Fig. 8. Aircraft 2, is the leader, and aircraft 1 and 3–9 are the followers. The matrix D in Eq. (20) was first calculated. Despite setting the number of connections equal to the number of degrees of freedom, D was not full rank. However, the optimal solution given by Eq. (22) did not require D to be full rank, so this did not present a difficulty. In Eq. (22), the weighting matrices are $W_\alpha = I_{2n}$ (the identity matrix) and $W_\eta = \eta I_N$, where η is a scalar weighting factor.

Table 1 Eigenvalues of closed-loop systems

Connection	Eigen value
Direct	$-0.0767 \pm 0.3300i$[a]
Nearest neighbor	$-0.0749 \pm 0.6735i$
	$-0.0749 \pm 0.6735i$
	$-0.0772 \pm 0.6146i$
	$-0.0772 \pm 0.6146i$
	$-0.0723 \pm 0.5862i$
	$-0.0723 \pm 0.5862i$
	$-0.0581 \pm 0.5026i$
	$-0.0581 \pm 0.5026i$
	$-0.0465 \pm 0.4482i$
	$-0.0465 \pm 0.4482i$
	$-0.0224 \pm 0.3297i$
	$-0.0224 \pm 0.3297i$
	$-0.0138 \pm 0.2661i$
	$-0.0138 \pm 0.2661i$
	$-0.0023 \pm 0.1146i$
	$-0.0023 \pm 0.1146i$
	$-0.0010 \pm 0.0816i$
	$-0.0010 \pm 0.0816i$

[a]For all 18 values.

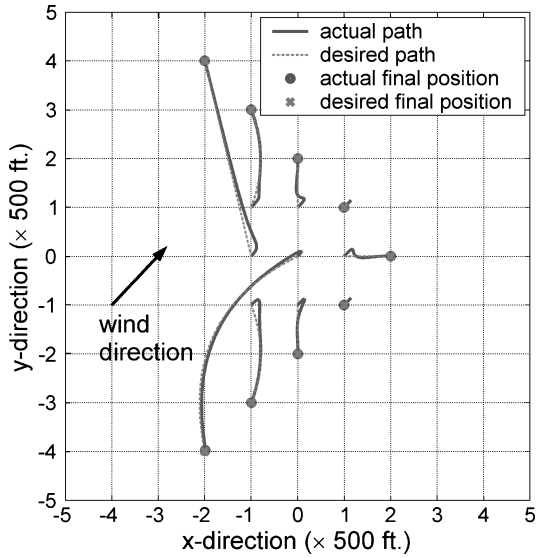

Fig. 7 Direct formation change in an initial wind gust.

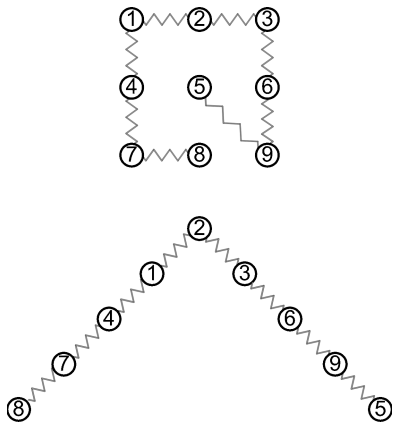

Fig. 8 Open connectivity.

The displacement feedback gains for nearest neighbor coordination were set equal to the displacement feedback gains for the direct coordination, that is, $g_k = g$ for each k. Of course, in direct coordination each aircraft is directly connected to the nominal path, whereas in nearest-neighbor coordination each aircraft is connected to its nearest neighbors. These differences are expected to be observed in the results. The velocity feedback gains were determined from Eq. (22), which is a linear approximation. The accuracy of the approximation

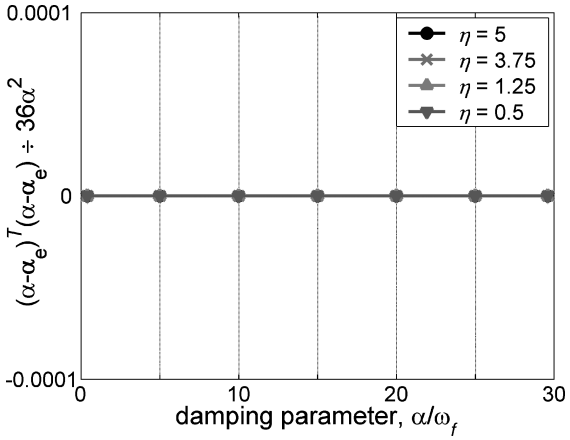

Fig. 9 Verification of accuracy of perturbation analysis.

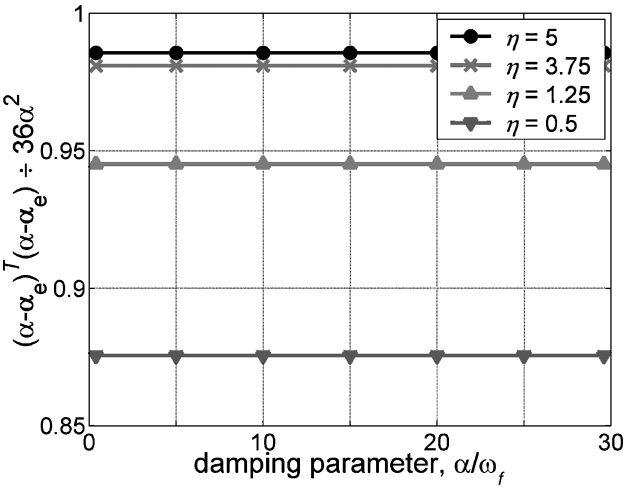

Fig. 10 Nonuniformity part of J.

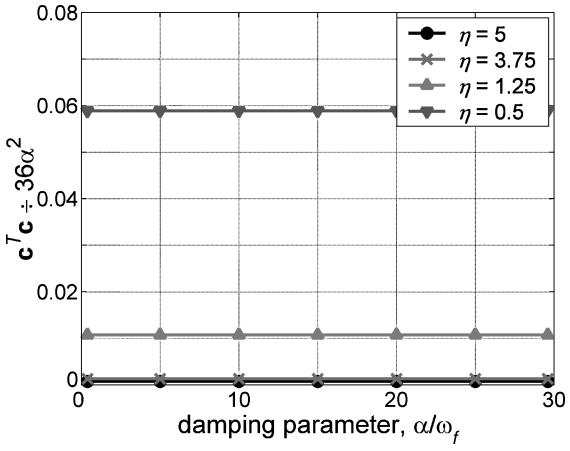

Fig. 11 Cost part of J.

was first examined in Fig. 9 over a range of damping factors. In Fig. 9, $\boldsymbol{\alpha}_e$ is the vector of exact decay rates that are obtained from the closed-loop eigenvalue problem associated with Eq. (16) and ω_f is the fundamental frequency of the system. Figure 9 shows that the approximation is accurate over the damping ratios α/ω_f of interest.

In this example, the level of nonuniformity of the decay rates was examined over a range of damping ratios and for different weighing parameters η. As shown in Fig. 10, the level of nonuniformity does not depend on the damping ratio, and it increases with η. Figure 11 shows the control effort over a range of damping ratios and for different weighing parameters η. Like the nonuniformity in Fig. 10, the control effort does not depend on the damping ratio, but it decreases with increasing η.

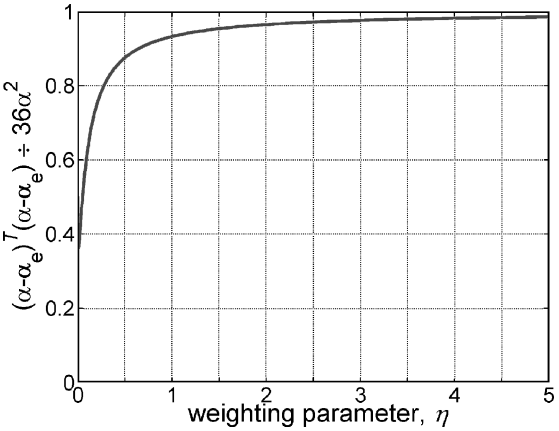

Fig. 12 Weighting parameter effect.

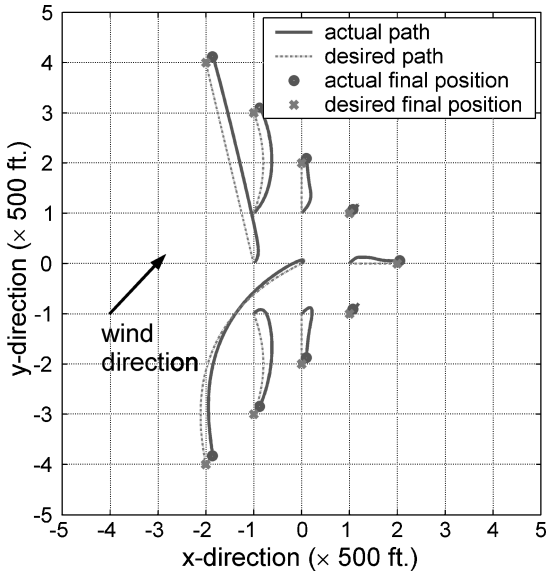

Fig. 13 Nearest-neighbor formation change in an initial wind gust.

Figures 12 shows that there is a practical nonzero minimum level of nonuniformity that is attainable, even when the control effort is allowed to increase to a prohibitively high level. The limit is a result of the rank deficiency of D. Table 1 shows that the nonuniformity in Fig. 12 is dominated by the lowest mode of vibration, which damps out at a lower rate than the other modes.

Figure 13 shows a formation change in which a wind gust causes the initial aircraft velocity to change by $v_w = 19$ kn, which is about one-half the size of the disturbance used for direct coordination (Fig. 8), although still quite large. The weighting parameter was set to $\eta = 0.001$, a very low value aimed at weighting uniformity over control effort (Fig. 12). Notice in Fig. 13 that the motion settled out in the specified time. The peak overshoot in the response was larger than the overshoot found in Fig. 8 for direct coordination, despite the smaller initial gust. The degradation in performance was smallest near the leader and was greatest in the back of the formation. As a general trend, the deviations of the final positions of the aircraft from the desired positions increase as the aircraft are farther from the leader. The relative displacement and velocity measurements become less effective feedback variables when they are located farther back in the formation.

VIII. Summary

Two important approaches to autonomous coordination of aircraft formations were studied. Well-known separation principles used in aircraft design were applied to the problem of coordinating formations. Both approaches are scalable to formations having a large number of aircraft. Separation principles were employed for 1) formation coordination and aircraft control, 2) signal transmission and reception, 3) tracking and regulation, 4) spatial and temporal tracking, 5) stiffening and damping, and 6) decentralized feedback connections (direct and nearest neighbor). In particular, the aircraft formation problem was separated into a two-level hierarchy associated with formation coordination and individual aircraft control. The focus of this paper was on the autonomous aircraft formation coordination problem. Equations (2) and (3) showed how to separate the autonomous formation coordination problem into a tracking problem and a regulation problem. Equation (8) further showed how to separate the tracking path into a spatial part and a temporal part. A straight path and a parabolic path were illustrated in Eqs. (10a–10c) and Eq. (11). It was then shown how to separate stiffening and damping in Eq. (13) for direct coordination and in Eq. (16) for nearest-neighbor coordination. In Eqs. (21) and (22), a simple way was developed to obtain control gains for nearest-neighbor coordination. In addition, the following conclusions about the relative merits of direct coordination and nearest-neighbor coordination were drawn:

1) Direct coordination is the preferred of the two approaches when the weight requirements of the inertial sensors are satisfied (which is difficult in microaerial aircraft) and when a reference source is available nearby, that is, when a reference signal of sufficiently low noise is available.

2) For fuel optimality, the closed-loop damping factors in the formation are bound from above by about 1.5.

3) Nearest-neighbor coordination could potentially be preferred when relative measurement information is desirable, for example, for collision avoidance.

4) The direct coordination approach is suited to short-distance problems where differential corrections are available.

5) The nearest-neighbor coordination approach is suited to long-distance problems, where differential corrections are not available.

6)When relative measurements are used, caution should be exercised because position errors propagate from the leader toward the back of the formation. Although not shown in the paper, this can be prevented by interspersing leaders throughout the formation.

Also several topics were introduced that would benefit from further study. Sets of elementary formations that possess attractive properties have not been developed, nor has a strategy for aircraft connectivity that minimizes tracking paths and maximizes separation distances between aircraft. This paper also was confined to two-way connections and single leaders; unanswered questions remain about the viability of one-way connections and the use of multiple leaders. Additional case studies showing the ability of flight control systems to maintain nominal conditions would also be useful.

Acknowledgment

This work was supported in part by NASA Grant NGT-1-00107.

References

[1]Balas, M. J., "Active Control of Flexible Systems," *Journal of Optimization Theory and Applications*, Vol. 25, No. 3, 1978, pp. 415–436.

[2]Meirovitch, L., and Baruh, H., "Control of Self-Adjoint Distributed-Parameter Systems," *Journal of Guidance, Control, and Dynamics*, Vol. 5, No. 1, 1982, pp. 60–66.

[3]Arbel, A., and Gupta, N. K., "Robust Collocated Control for Large Flexible Space Structures," *Journal of Guidance, Control, and Dynamics*, Vol. 4, No. 5, 1981, pp. 480–486.

[4]Hale, A., and Rahn, G. A., "Robust Control of Self-Adjoint Distributed-Parameter Systems," *Journal of Guidance, Control, and Dynamics*, Vol. 7, No. 3, 1984, pp. 265–273.

[5]Baruh, H., and Silverberg, L., "Robust Natural Control of Distributed Systems," *Journal of Guidance, Control and Dynamics*, Vol. 8, No. 6, 1985, pp. 717–724.

[6]Calico, R. A., and Miller, W. T., "Decentralized Control for a Flexible Spacecraft," AIAA Paper 82-1404, Aug. 1983.

[7]Meirovitch, L., and Silverberg, L., "Globally Optimal Control of Distributed Systems," *Journal of Optimal Control Applications and Methods*, Vol. 4, June 1983, pp. 365–386.

[8]Silverberg, L., "Uniform Damping Control of Spacecraft," *Journal of Guidance, Control, and Dynamics*, Vol. 9, No. 2, 1983, pp. 221–227.

[9]Silverberg, L., and Morton, M., "On the Nature of Natural Control," *Journal of Vibration, Acoustics, Stress and Reliability in Design*, Vol. 111, Oct. 1989, pp. 412–422.

[10]Silverberg, L., "Motion Control of Space Structures," *Journal of Aerospace Engineering*, Vol. 3, No. 4, 1990, pp. 223–234.

[11]Silverberg, L., Redmond, J., and Weaver, L., Jr., "Uniform Damping Control: Discretization and Optimization," *Journal of Applied Mathematical Modeling*, Vol. 16, No. 3, 1992, pp. 133–140.

[12]Baruh, H., and Silverberg, L., "Simultaneous Maneuver and Vibration Suppression of Flexible Spacecraft," *Journal of Applied Mathematical Modeling*, Vol. 12, No. 6, 1988, pp. 546–555.

[13]Silverberg, L., and Foster, L. A., "Decentralized Feedback Maneuver of Flexible Spacecraft," *Journal of Guidance, Control, and Dynamics*, Vol. 13, No. 2, 1990, pp. 258–264.

[14]Silverberg, L., and Washington, G., "Uniform Damping and Stiffness Control of Structures with Distributed Actuators," *Journal of Dynamic Systems, Measurement and Control*, Vol. 119, No. 3, 1997, pp. 561–565.

[15]Silverberg, L., and Washington, G., "Weighted-Residual Discretization for Uniform Damping and Uniform Stiffening of Structural Systems, *Journal of Guidance, Control, and Dynamics*, Vol. 22, No. 4, 1999, pp. 614–618.

[16]Wolfe, J. D., Chichka, D. F., and Speyer, J. L., "Decentralized Controllers for Unmanned Aerial Vehicle Formation Flight," AIAA Paper 96-3833, July 1996.

[17]Pachter, M., D'Azzo, J. J., and Proud, A. W., "Tight Formation Flight Control," *Journal of Guidance, Control, and Dynamics*, Vol. 24, No. 2, 2001, pp. 246–254.

[18]Richards, A., Bellingham, J., Tillerson, M., and How, J. P., "Coordination and Control of Multiple UAVs," AIAA Paper 2002-4588, Aug. 2002.

[19]Bellingham, J., Tillerson, M., Alighanbari, M., and How, J. P., "Cooperative Path Planning of Multiple UAVs in Dynamics and Uncertain Environments," *Institute of Electrical and Electronics Engineers Conference on Decision and Control*, Vol. 3, Dec. 2002, pp. 2816–2822.

[20]Mehiel, E. A., and Balas, M. J., "A Rule Based Algorithm that Produces Exponentially Stable Formations of Autonomous Agents," AIAA Paper 2002-4591, Aug. 2002.

[21]Olsen, E., Park, C. W., and How, J. P., "3D Formation Flight Using Differential Carrier-Phase GPS Sensors," *Journal of Institute of Navigation*, Vol. 146, No. 1, 1999, pp. 35–48.

[22]Frazier, J. W., and Gopalarathnam, A., "Optimum Downwash Behind Wings in Formation Flight," *Journal of Aircraft*, Vol. 40, No. 4, 2003, pp. 799–803.

[23]Meirovitch L., *Dynamics and Control of Structures*, Wiley, New York, 1990.

[24]Meirovitch, L., *Principles and Techniques of Vibrations*, Prentice–Hall, Upper Saddle River, NJ, 1997.

[25]Lawson, C. L., and Hanson, R., *Solving Least Squares Problems*, Prentice–Hall, Englewood Cliffs, NJ, 1974.

[26]Nelson, R. C., *Flight Stability and Automatic Control*, McGraw–Hill, New York, 1989.